Andean Geology 43 (1): 1-19. January, 2016
doi: 10.5027/andgeoV43n1-a01

Andean Geology
www.andeangeology.cl

Holocene tephrochronology around Cochrane (~47° S), southern Chile

Charles R. Stern[1], Patricio I. Moreno[2], William I. Henríquez[2], Rodrigo Villa-Martínez[3], Esteban Sagredo[4], Juan C. Aravena[3], Ricardo de Pol-Holz[3]

[1] *Department of Geological Sciences, University of Colorado, Boulder, Colorado, 80309-0399, USA. charles.stern@colorado.edu*

[2] *Instituto de Ecología y Biodiversidad, Departamento de Ciencias Ecológicas, Universidad de Chile, Casilla 653, Santiago, Chile. pimoreno@u.uchile.cl; willybgo@ug.uchile.cl*

[3] *GAIA-Antártica, Universidad de Magallanes, Avda. Bulnes 01855, Punta Arenas, Chile. rodrigo.villa@umag.cl; juan.aravena@umag.cl; ricardo.depol@umag.cl*

[4] *Instituto de Geografía, Facultad de Historia, Geografía y Ciencia Política, Pontificia Universidad Católica de Chile, Avda. Vicuña Mackenna 4860, Santiago, Chile. esagredo@uc.cl*

ABSTRACT. Two Holocene tephras encountered in outcrops, cores and trenches in bogs, and lake cores in the area around Cochrane, southern Chile, are identified (based on their age, tephra glass color and morphology, mineralogy, and both bulk and glass chemistry) as H1 derived from Hudson volcano, and MEN1 derived from Mentolat volcano. New AMS radiocarbon ages indicate systematic differences between those determined in lake cores (MEN1=7,689 and H1=8,440 cal yrs BP) and surface deposits (MEN1=7,471 and H1=7,891 cal yrs BP), with the lake cores being somewhat older. H1 tephra layers range from 8 to 18 cm thick, suggesting that both the area of the 10 cm isopach and the volume of this eruption were larger than previously suggested, but not greatly, and that the direction of maximum dispersion was more to the south. MEN1 tephra layers range from 1-4 cm in thickness, indicating that this was probably a reasonably large (>5 km^3) eruption. Some of the lake cores also contain thin layers (<2 cm) of late Holocene H2 tephra and the recent H3 (1991 AD) tephra, both derived from the Hudson volcano. No tephra evidence has been observed for any late Pleistocene tephra, nor for the existence of the supposed Arenales volcano, proposed to be located west of Cochrane.

Keywords: Tephra, Tephrochronology, Volcanism, Hudson, Mentolat, Andes, Chile.

RESUMEN. Tefrocronología holocénica cerca de Cochrane (~47° S), Chile Austral. Dos tefras holocenas reconocidas en afloramientos testigos y trincheras en pantanos y lagos de la zona de Cochrane, Chile, han sido identificadas (sobre la base de su edad, color y morfología de las partículas vítreas, mineralogía y composición química de la roca total y del vidrio) como H1 y MEN1, provenientes de los volcanes Hudson y Mentolat, respectivamente. Nuevas edades radiocarbónicas AMS asociadas a estas tefras revelan diferencias sistemáticas entre los testigos lacustres (MEN1=7,689 y H1=8,440 años cal. AP) y los depósitos en superficie (MEN1=7,471 y H1=7,891 años cal. AP), en que las edades en los testigos lacustres son algo más antiguas. Los horizontes de la tefra H1 varían entre 8 y 18 cm de espesor, lo que indicaría que tanto el área de la isópaca de 10 cm como el volumen de esta erupción fue levemente mayor a lo previamente reconocido, y que la dirección de dispersión fue más hacia el sur. Los niveles de la tefra MEN1 varían entre 1 y 4 cm de espesor, lo que sugiere que esta fue una erupción relativamente grande (>5km^3). Algunos testigos lacustres también incluyen niveles más finos (<2 cm) de otra tefra (H2) del Holoceno tardío y de la tefra asociada a la erupción del año 1991, ambas derivadas del volcán Hudson. No se encontraron evidencias de tefras pleistocénicas tardías ni tampoco de la presencia del volcán Arenales, supuestamente ubicado al oeste de Cochrane y cuya existencia ha sido puesta en duda.

Palabras clave: Tefra, Tefrocronología, Volcanismo, Hudson, Mentolat, Andes, Chile.

1. Introduction

The town of Cochrane, in the region of Aysén, southern Chile (Figs. 1 and 2), occurs within the volcanic gap between the Hudson volcano, at the southernmost end of the Andean Southern Volcanic Zone (SVZ), and Lautaro volcano at the northernmost end of the Austral Volcanic Zones (AVZ) to the south (Stern, 2004; Stern *et al*., 2007). However, it has also been suggested, but never confirmed, that there is a possible volcano Arenales in this volcanic gap (47.2° S; 73.5° W; Fig. 1) to the west of Cochrane (Lliboutry, 1999).

Although Cochrane occurs in a region without active volcanoes, tephra deposits derived from explosive eruptions of volcanoes in the southernmost

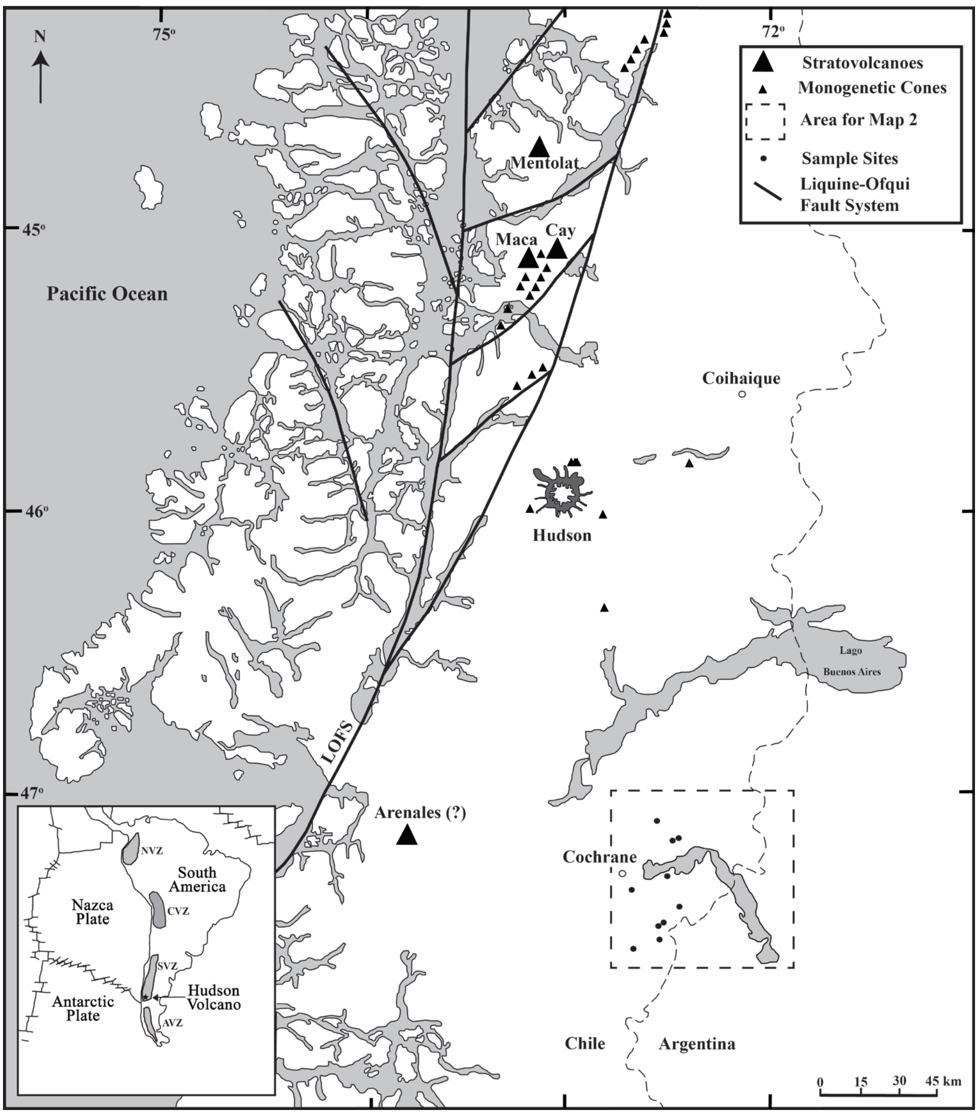

FIG. 1. Regional map showing the location of Cochrane relative to the volcanoes at the southern end of the SVZ. Also shown are the locations of some of the monogenetic centers along the Liquiñe-Ofqui Fault System (LOFS) and surrounding Hudson (Gutiérrez *et al*., 2005; Vargas *et al*., 2013), and the proposed location of the Arenales volcano (Lliboutry, 1999), the existence of which has not yet been confirmed. Boxed area near Cochrane is the locations of the road-cuts, trenches and cores containing the tephra layers described in the text.

FIG. 2. Map showing the locations of the road-cut outcrop (Fig. 3), the four pits (Fig. 4) in bogs, the Anónima bog which was cored, and the four lakes (Fig. 5) from which tephras were collected (Table 1). Also shown are the location of two sites (TCHA-10 and TCHA-47) at which H1 tephra was dated by Gardeweg and Sellés (2013).

SVZ have been described in lake sediment cores and outcrops from this area. Villa-Martínez *et al*. (2012) described two tephra in a sediment core from Augusta Lake located 25 km northeast of Cochrane (Fig. 2), which they identified as being derived from the H1 eruption of Hudson volcano (Naranjo and Stern, 1998) and the MEN1 eruption of Mentolat volcano (Naranjo and Stern, 2004). Gardeweg and Sellés (2013) also described various outcrops of tephra deposits in the area of Cochrane which they attributed to both the H1 and younger H2 eruptions of Hudson. The data of Gardeweg and Sellés (2013) suggest that both these eruptions were significantly larger than previously estimated by Naranjo and Stern (1998). More recently McCulloch *et al*. (2014) also reported both H1 and MEN1 tephra from a bog sediment core at La Frontera in Argentina, 70 km northeast of Cochrane.

All these recent results are consistent with the previous conclusions of Stern (1991, 2008) and Naranjo and Stern (1998, 2004) that the H1 and H2 eruptions of Hudson and MEN1 of Mentolat, along with the older Ho (Weller *et al*., 2014) and younger H3 (1991 AD; Scasso *et al*., 1994) eruptions of Hudson, were among the largest Holocene explosive events generated by the volcanoes in the southern SVZ. The tephra deposits produced by all these eruptions have already and will continue to provide important chronological markers for archaeologic (Prieto *et al*., 2013) and paleoclimate (Waldmann *et al*., 2009; Borromei *et al*., 2010; Unkel *et al*., 2010; Hermanns and Biester, 2011; Björck *et al*., 2012; Villa-Martínez *et al*., 2012; Menounos *et al*., 2013; McCulloch *et al*., 2014) studies in southern Patagonia. For these reasons, as well as being significant for evaluating volcanic risks and hazards for the inhabitants of

FIG. 3. Photo of the ~12 cm thick Hudson H1 tephra from near the road-cut PC14-01-06 (Fig. 2).

Cochrane and other population centers in southern Chile, further study of tephra deposits produced by these large explosive eruptions are important for refining our understanding of their size, age and the distribution of the pyroclastic products they produce.

Here we describe four different Holocene tephra layers, which occur in road-cut outcrops (Fig. 3), cores and trenches (Fig. 4) in bogs, and lacustrine sediment cores (Fig. 5) collected from four small lakes (Edita, Maldonado, Augusta, and Pepa; Fig. 2) in this area (Table 1). Our new chronologic and petrochemical data indicate that these tephra are derived from the previously identified large eruptions H1, H2 and H3 of Hudson and MEN1 of Mentolat volcanos, and that these tephra provide no evidence for the existence of the Arenales volcano.

2. Methods

Tephra samples were collected from a road-cut exposure (Fig. 3), one core and four hand-dug trenches (Fig. 4) in bogs, and sediment cores (Fig. 5) from four small lakes within spatially limited water-shed basins selected to minimize the amount of inorganic sediment deposited in the lakes (Table 1). The lake sediment cores were obtained using a 5-cm-diameter modified Livingstone piston corer (Wright, 1967). X-ray images of the cores (Fig. 5) were taken to allow for better visual identification of the tephra deposits and to provide a means of stratigraphic correlation of the tephra layers between the cores. The white layers in these images are the denser lithologies, often tephra deposits, but in some cases

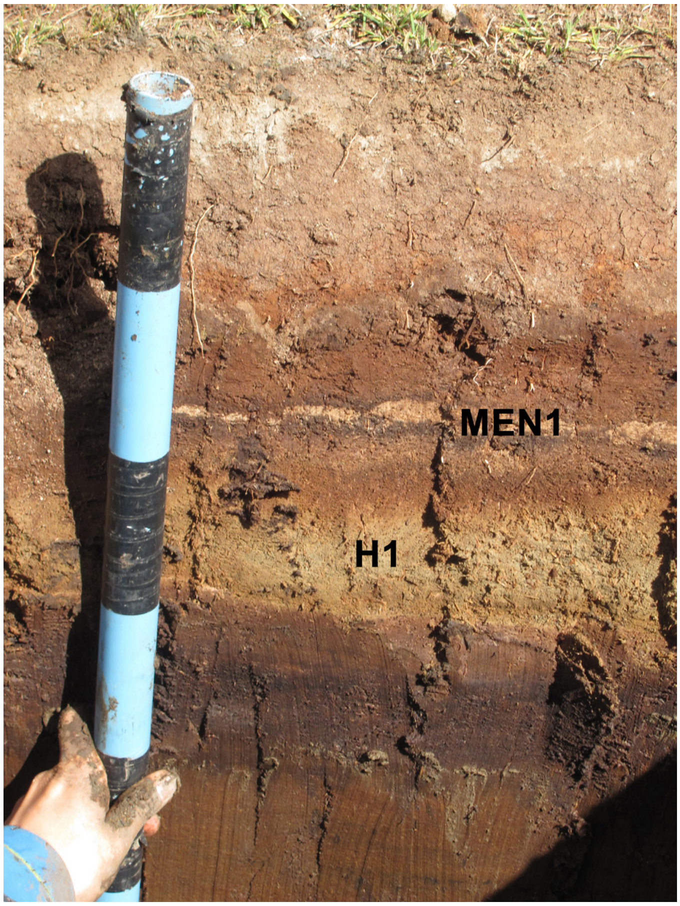

FIG. 4. Photo of 2 cm thick Mentolat MEN1 tephra (sample PC14-01-46) and 10 cm thick H1 tephra (PC14-01-44) from a pit ~30 km southeast of Cochrane (Fig. 2; Table 1). Each blue and black band on the pole are 10 cm in length.

sand (Fig. 5), and the darker layers are less dense organic-rich lacustrine sediments. The chronology of the tephra in the trenches and cores is controlled by AMS radiocarbon dates of organic material in the overlying and underlying sediments (Tables 2 and 3). In the tables, the ages from the lake deposits are separated from those from surface deposits in bogs. Radiocarbon dates were converted to calendar years before present (cal yrs BP) using the CALIB 7 program and the SHCal13 dataset (Stuiver *et al*., 1998; Hogg *et al*., 2013).

The tephra samples were washed to remove any organic matter, and then dried and sieved to remove any coarse fraction material not volcanic in origin. After cleaning, the bulk tephra samples were mounted on petrographic slides to examine under a petrographic microscope in order to identify petrographic characteristics such as tephra glass color and morphology and the identity of mineral phases (Fig. 6). The major element compositions of 2 samples of bulk tephra (Table 4) were determined by Activation Laboratories, Canada. Trace-element data for bulk tephra samples (Tables 5-7) were determined using an ELAN D CR ICP-MS at the University of Colorado. Trace-element compositions are considered accurate to ±5% at the level of concentrations in these samples, based on repeated analysis of standard rock samples of known composition (Saadat and Stern, 2011). The major element compositions of tephra glasses (Table 4) were determined using a Jeol JXA-733 Electron Microprobe operating at 15 KV accelerating potential with a 10 nA probe current and a 5-10 µm diameter beam to minimize volatilization of sodium.

FIG. 5. X-ray image of ~10 meter long core PC0902A from Lago Edita (Fig. 2), showing bright white relatively high density H1, H2 and MEN1 tephra layers within darker lower density organic-rich lacustrine sediments. Core is divided into 10 segments each approximately 1 meter long. Bright bands are dense layers which include tephra H2 in segment #4 and MEN1 and H1 in segment #7. H1 tephra is ~14 cm thick, MEN1 ~3 cm thick and H2 only ~1 cm. Higher density (brighter) laminated material in the deeper part of the core (segments #8-10) below H1 and MEN1 is glacial-lacustrine clay, silt and sand. Bright band marked with X in segment #6 is also sand, not tephra.

3. Results

Thickness (Table 1), radiocarbon ages (Tables 2 and 3), and petrochemical information, including tephra glass color and morphology (Figs. 6), as well as mineralogy, bulk tephra major (Table 4) and trace-element chemistry (Tables 5-7), and tephra glass compositions (Table 4), indicate, by comparison with previously described tephra from farther north, that the four different tephra layers were derived from three different large explosive eruptions of the Hudson volcano (H1, H2 and H3; Naranjo and Stern, 1998) and one from the Mentolat volcano (MEN1; Naranjo and Stern, 2004). No late Pleistocene tephra were encountered in the lake cores, some of which, such as the core from Augusta lake, preserve a record that extends back in time to over 19,500 cal yrs BP (Villa-Martínez *et al*., 2012). The results are described in more detail below in the order from the oldest to the youngest tephra.

TABLE 1. LOCATION OF LAKES, BOGS AND OUTCROPS WITH TEPHRA NEAR COCHRANE.

				Tephra thickness cm	
Lake cores		**Latitude °S**	**Longitude °W**	**H1**	**MEN1**
Augusta	PC0903B	47°4’17.60”	72°22’31.01”	8	4
Edita	PC0902A	47°9’5.40”	72°21’12.50”	14	3
Pepa	PC0901A	47°9’0.55”	72°20’28.81”	14	3
Maldonado	PC0904A	47°15’45.91”	72°31’11.57”	8	2
Bog cores					
Anónima	PC0607B	47°14’43.80”	72°22’22.89”	8	2
Bog excavations					
PC14-01-11/14	-	47°29’1.94”	72°22’19.55”	10	2
PC14-01-25/30	-	47°26’57.97”	72°23’15.36”	18	1
PC14-02-06/10	-	47°23’52.62”	72°20’17.23”	10	1
PC14-01-44/46	-	47°29’12.51”	72°22’58.53”	10	2
Outcrops					
PC14-01-6	-	47°29’10.64”	72°30’31.79”	12	X

3.1. H1 tephra

The oldest and thickest (8-18 cm) tan to orange-brown tephra layers in the road-cut, trenches and lake cores near Cochrane are chronologically constrained by 10 new AMS radiocarbon ages (one from the road-cut outcrop PC14-01-06, four from the two bog trenches PC14-02-06 and PC14-01-14, and five in the cores from Edita, Pepa and Maldonado lakes; Table 2). The minimum AMS ages from these three lakes, and other lakes elsewhere in Patagonia where H1 have been dated, range between 7,525±20 to 7,715±60 ^{14}C yrs BP, the maximum ages between 7,750±50 and 7,775±60 ^{14}C yrs BP, and their average is 7,683±33 ^{14}C yrs BP (median probability age: 8,440 cal yrs BP; Table 2). The AMS ages from these three surface deposits, and other surface deposits in Patagonia, are systematically lower than the ages from the lake cores, with minimum ages ranging from 6,755±40 to 7,176±19 ^{14}C yrs BP, maximum ages from 6,750±25 to 7,410±25 ^{14}C yrs BP, and an average age of 7,084±23 ^{14}C yrs BP (median probability age: 7,891 cal yrs BP; Table 2). Although this average is older than the average obtained in the previous most recent compilation of H1 ages (6,890 ^{14}C yrs BP; Prieto *et al*., 2013), this new compilation includes only AMS radiocarbon ages (Table 2) and not any conventional ages. The <200 year difference between the average of these new AMS ages and the previous compilation of conventional ages is nevertheless consistent with these tephra having been generated by the H1 eruption of Hudson.

These tephra layers all contain dominantly brown glass with abundant stretched vesicles (Fig. 6A). Mineral grains include plagioclase, orthopyroxene and clinopyroxene. Bulk tephra major element oxide chemistry (Table 4) indicates that these tephra are andesitic (SiO_2 of 62 wt%), with relatively high TiO_2 (1.4 wt%), Na_2O (5.6 wt%), and K_2O (2.6 wt%), as are tephra glass compositions (Fig. 7). Trace-element analysis (Table 5; Fig. 8) of bulk tephra samples from the lake cores indicate that these tephra, as well as the tephra in three of the bog trenches, the bog core and that collected from the outcrop, all have elevated concentrations of Ti (9,189-10,246 ppm), Rb (38-50 ppm), Zr (288-417 ppm), Ba (604-807 ppm), La (35.0-43.7 ppm) and Yb (3.1-4.8 ppm). These compositions are similar to other samples of lavas and tephra from Hudson volcano (Fig. 8) and distinct from the products of the other large stratovolcanoes (Maca, Cay and Mentolat) in the southernmost SVZ.

Their age, thickness, and all these petrochemical characteristics together indicate that these tephra were produced by the H1 eruption of the Hudson volcano (Stern, 1991, 2008; Naranjo and Stern, 1998).

TABLE 2. NEW AND PREVIOUSLY PUBLISHED AMS AGES FOR H1 TEPHRA FROM COCHRANE AREA AND ELSEWHERE.

Location	Lake	Core	depth cm	Sample Code	^{14}C age	error	median probability	lower cal range BP	upper cal range BP	reference
Cores from lakes										
Minumum ages (above H1)										
Cochrane	Pepa	PC0901DT2	39-40	UCIAMS-133392	7,525	20	8,316	8,202	8,377	this paper
Cochrane	Edita	PC0902AT7	18-19	UCIAMS-133415	7,600	25	8,379	8,333	8,414	this paper
Cochrane	Maldonado	PC0904BT6	8-9	UCIAMS-133397	7,565	20	8,358	8,216	8,402	this paper
Isla de los Estados	Cascadia	-	387	LuS6935	7,715	60	8,471	8,382	8,584	Unkel *et al.*, 2010
Average minimum					**7,565**	**31**	**8,385**	**8,368**	**8,403**	
Maximum ages (below H1)										
Cochrane	Pepa	PC0901DT2	50-51	UCIAMS-133393	7,750	25	8,489	8,415	8,555	this paper
Cochrane	Maldonado	PC0904BT6	21-22	UCIAMS-133398	7,770	20	8,502	8,429	8,580	this paper
Isla de los Estados	Cascadia	-	391	LuS6936	7,775	60	8,510	8,404	8,627	Unkel *et al.*, 2010
Average maximum					**7,763**	**35**	**8,558**	**8,480**	**8,592**	
Average all lake cores					**7,683**	**33**	**8,440**	**8,423**	**8,462**	

Location	Name	Sample No.	depth cm	Sample Code	^{14}C age	error	median probability	lower cal range BP	upper cal range BP	reference
Trenches and outcrops from surface (bog) deposits										
Minumum ages (above H1)										
Isla de los Estados	Galvarne bog	-	449,5	-	6,755	40	7,578	7,435	7,687	Bjork *et al.*, 2012
Cochrane	PC14-02-06/10	-	-	-	6,885	13	7,671	7,606	7,746	this paper
Cochrane	PC14-01-11/14	-	-	-	6,955	13	7,738	7,675	7,825	this paper
Tierra del Fuego	Cotorras bog	-	470-475	AA62823	7,043	24	7,837	7,709	7,938	Borromei *et al.*, 2010
Cochrane	road cut	-	-	-	7,165	30	7,948	7,793	8,149	A. Holz, per comm 2011
Santa Cruz, Arg	La Frontera	-	-	SUERC-49366	7,176	19	7,961	7,859	8,024	McCulloch *et al.*, 2014
Average minimum					**6,978**	**23**	**7,814**	**7,749**	**7,916**	
Maximum ages (below H1)										
Isla de los Estados	Galvarne bog	-	454,5	LuS9301	6,750	25	7,576	7,482	7,666	Bjork *et al.*, 2012
Cochrane	PC14-01-11/14	-	-	-	6,980	30	7,772	7,663	7,931	this paper
Cochrane	General Carrera lake	TCHA-43A	-	-	7,010	25	7,800	7,685	7,930	Gardeweg and Sellés 2013
Cochrane	PC14-02-06/10	-	-	-	7,045	20	7,841	7,722	7,938	this paper
Cochrane	Tranquilo river	TCHA-10A	-	-	7,220	25	7,995	7,874	8,159	Gardeweg and Sellés 2013
Magallanes	Hambre lake	-	804-806	Keck79260	7,370	10	8,115	8,035	8,188	Hermanns and Biester 2011
Cochrane	PC14-01-06	-	-	-	7,405	20	8,181	8,042	8,315	this paper
Cochrane	Chacabuco bridge	TCHA-47A	-	-	7,410	25	8,189	8,038	8,326	Gardeweg and Sellés 2013
Average maximum					**7,241**	**23**	**8,036**	**8,001**	**8,154**	
Average all surface deposits					**7,084**	**23**	**7,891**	**7,865**	**7,919**	

TABLE 3. NEW AND PREVIOUSLY PUBLISHED AMS AGES FROM MEN1 TEPHRA FROM COCHRANE AREA AND ELSEWHERE.

Lake	Core	depth cm	Sample Code	^{14}C age	error	median probability	lower cal range BP	upper cal range BP	reference
Cores from lakes									
Minimum ages (above MEN1)									
Pepa	PC0901DT2	23-24	UCIAMS-133390	6,745	20	7,575	7,507	7,618	this paper
Augusta	PC0903BT2	1106	UCIAMS-146710	6,770	40	7,594	7,509	7,670	this paper
Edita	PC0902AT7	627	UCIAMS-133395	6,990	25	7,773	7,685	7,911	this paper
Maldonado	PC0904BT5	52-53	UCIAMS-133413	6,860	20	7,649	7,594	7,689	this paper
Average minimum				**6,841**	**26**	**7,674**	**7,626**	**7,692**	
Maximum ages (below MEN1)									
			UCIAMS-133391	6,900	20	7,684	7,616	7,756	this paper
			UCIAMS-133413	6,860	20	7,649	7,594	7,689	this paper
			UCIAMS-133394	6,910	20	7,694	7,624	7,785	this paper
			UCIAMS-133396	6,910	20	7,694	7,624	7,785	this paper
Average maximum				**6,895**	**20**	**7,709**	**7,677**	**7,756**	
Average all lake cores				**6,872**	**23**	**7,689**	**7,669**	**7,722**	
Location		**Sample number**							
Trenches and outcrops of bog deposits									
Maximum ages (below MEN1)									
PC14-01-11/14		PC14-01-12	Beta-279574	6,520	40	7,380	7,290	7,469	this paper
Simpson River		94T-58A	-	6,690	60	7,527	7,430	7,613	Naranjo and Stern 2004
Average maximum				**6,572**	**50**	**7,471**	**7,427**	**7,560**	

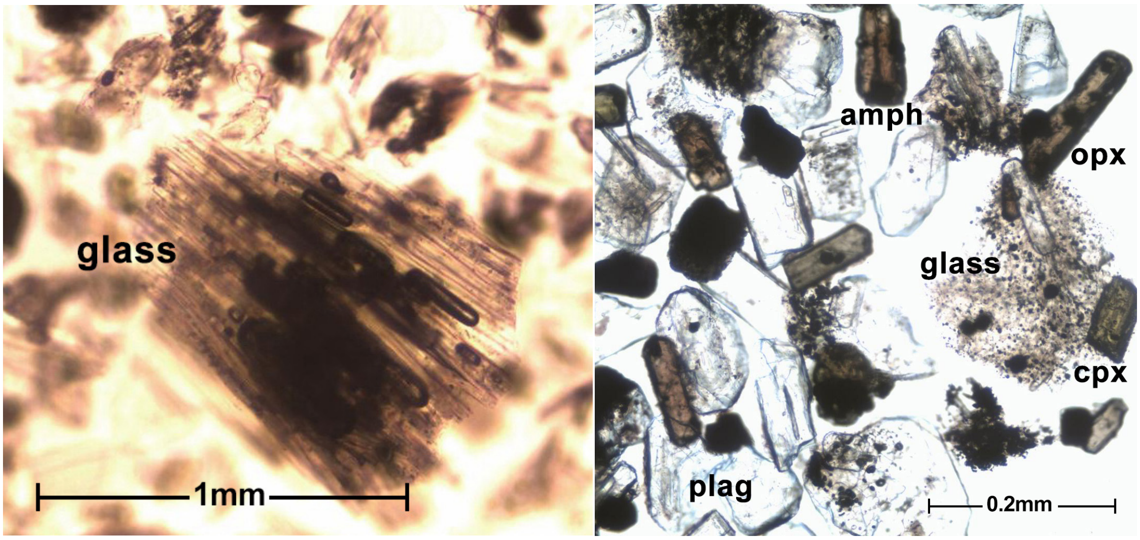

FIG. 6. Photomicrographs of **A.** Hudson H1 tephra containing brown glass shards, with abundant stretched vesicles, and few crystals; **B.** Crystal-rich Mentolat MEN1 tephra containing clear glass, plagioclase, orthopyroxene, clinopyroxene and minor amphibole.

TABLE 4. COMPOSITIONS OF H1 AND MEN1 BULK TEPHRA AND TEPHRA GLASSES.

Source	Hudson			Mentolat		
	Bulk		Glass	Bulk		Glass
tephra	H1	H1	H1	MEN1	MEN1	MEN1
	Edita	94T-44*	Edita	PC14 01-25	94T-36*	PC14 01-25
SiO_2	62.15	61.12	63.72	60.80	56.94	71.05
TiO_2	1.41	1.52	1.26	0.86	1.34	0.49
$Al2O_3$	16.24	16.00	16.48	18.51	16.38	14.99
Fe_2O_3(T)	4.97	5.39	5.02	4.69	7.67	2.90
MnO	0.16	0.18	0.15	0.12	0.18	0.09
MgO	1.69	1.89	1.46	1.63	4.49	0.68
CaO	3.65	3.78	3.12	6.07	5.64	2.78
Na_2O	5.60	5.61	5.27	4.50	3.91	5.21
K_2O	2.57	2.37	2.89	0.74	0.80	1.44
P205	0.32	0.36	0.31	0.14	0.11	0.07
LOI	1.18	1.60	-	1.51	1.91	-
Total	99.94	99.87	99.68	99.87	99.08	99.70

* Naranjo and Stern (1998, 2004).

3.2. MEN1 tephra

The somewhat younger and thinner (1-4 cm) white tephra layers in the trenches (Fig. 4) and cores (Fig. 5) are chronologically constrained by 9 new AMS ages (one from the trench PC14-01-11 and eight from the four lakes Edita, Pepa, Maldonado and Augusta; Table 3). The minimum ages for these

TABLE 5. TRACE-ELEMENT COMPOSITION OF HUDSON H1 TEPHRA IN THE VICINITY OF COCHRANE.

	Outcrop	Bog trenches and cores				Lake cores			
	PC14	PC14	PC14	PC14	Anonima	Pepa	Edita	Maldonado	
	01-06	02-06	01-14	01-30	0607B T9	0901A T1	0902A-T7	0608A T1	0904B T6
					60-66 cm	22-36 cm	20-38 cm	18-26 cm	27-35 cm
Lab #	CS 8015	CS 8014	CS 8019	CS 8020	CS-3050a	CS-3002	CS-3005	CS-1030	CS 1031
Ti	10,246	9,326	9,491	9,697	9,498	9,506	9,189	9,800	9,844
Mn	1,563	1,153	1,110	1,154	1,381	1,093	1,147	1,160	1,393
Rb	38	43	43	44	45	47	50	44	46
Sr	454	436	439	474	451	364	387	502	472
Y	42	44	42	39	36	41	44	33	39
Zr	367	342	379	350	288	370	417	293	313
Nb	17	16	23	16	14	18	19	17	16
Cs	0.8	1.1	1.3	1.0	0.9	1.4	1.3	0.9	1.1
Ba	807	736	793	666	650	604	702	713	635
Hf	8.1	7.9	10.7	8.1	6.5	9.2	8.8	8.4	6.5
Pb	10.6	9.8	10.6	9.6	7.8	9.7	9.7	9.4	9.3
Th	6.1	5.5	8.2	5.5	5.0	6.9	6.8	7.4	4.8
U	2.0	1.4	1.5	1.4	1.2	1.3	1.6	1.6	1.1
La	40.0	35.6	38.6	40.0	36.2	41.5	43.7	35.7	35.0
Ce	97.7	80.0	88.8	88.3	75.5	92.9	96.4	72.3	79.2
Pr	11.3	10.1	11.0	11.0	9.87	11.3	12.1	10.1	10.1
Nd	46.5	40.2	43.4	43.9	42.2	43.9	49.2	40.7	43.7
Sm	9.77	8.45	9.37	9.18	8.21	9.48	10.25	7.83	8.68
Eu	3.17	3.15	3.04	2.74	2.47	2.87	2.82	2.51	2.72
Gd	11.3	9.64	10.9	10.7	9.4	11.8	12.0	7.41	9.5
Tb	1.36	1.18	1.33	1.32	0.97	1.45	1.47	1.18	1.28
Dy	8.09	7.31	7.63	7.43	7.36	7.84	8.36	6.23	6.88
Ho	1.55	1.34	1.45	1.44	1.40	1.53	1.64	1.34	1.39
Er	4.70	4.21	4.82	4.53	4.26	4.69	5.25	3.77	4.07
Tm	0.60	0.58	0.62	0.59	0.58	0.64	0.68	0.54	0.55
Yb	4.30	4.01	4.21	4.23	3.78	4.46	4.68	3.14	3.67
Lu	0.58	0.51	0.62	0.58	0.53	0.67	0.72	0.61	0.55

tephra from the lake cores range between 6,745±20 to 6,860±20 ^{14}C yrs BP, the maximum ages between 6,900±20 and 6,910±20 ^{14}C yrs BP, and their average is 6,872±23 ^{14}C yrs BP (median probability age: 7,689 cal yrs BP; Table 3). As for H1, the ages from surface (bog) deposits are systematically lower than the ages from the lake cores, with maximum ages from 6,520±40 to 6,690±60 ^{14}C yrs BP and an average age of 6,572±50 ^{14}C yrs BP (median probability age: 7,471 cal yrs BP; Table 3). Nevertheless, both sets of ages are consistent with this being the same MEN1 tephra previously described by Naranjo and Stern, 2004)

These tephra are crystal-rich, with plagioclase, orthopyroxene, minor amphibole and clinopyroxene,

TABLE 6. TRACE-ELEMENT COMPOSITIONS OF MENTOLAT MEN1 TEPHRA FROM THE VICINITY OF COCHRANE AND ELSEWHERE.

Location	Near Cochrane								Elsewhere		
Trenches and cores in bogs						Lake cores			Cores		Outcrops
	PC14	PC14	PC14	Anónima	Anónima	Pepa	Edita	Maldo-nado	Mellizas	Embudo	Aisen
	01-25	01-46	01-11	0607B T9	0607B T9	0901A T1	0902A T7	0904B T5	1106A T4	EE0110A T7	T-36
	bulk	bulk	bulk	10-12 cm	10-12 cm	0-3 cm	4-7 cm	54-56 cm	54-56 cm	27-28 cm	
Lab #	CS 8013	CS8010	CS 8016	CS-3051	CS-1032	CS-3001	CS-3004	CS-1033	CS2022	CS5052	N&S 2004
Ti	3,214	4,156	3,713	2,923	3,010	2,594	2,672	3,659	4,233	4,852	5,932
Mn	877	868	836	759	798	618	698	843	991	1,070	964
Cs	1.2	1.2	1.3	1.8	1.5	2.0	2.1	1.9	1.2	0.9	-
Rb	17	15	19	23	24	20	24	23	15	22	18
Sr	414	448	444	324	426	383	370	411	418	393	416
Ba	233	250	272	289	275	272	295	285	227	298	-
Y	23	18	23	23	22	22	25	23	20	21	19
Zr	122	142	151	152	135	160	149	160	89	117	95
Nb	5	4	5	5	5	8	6	6	4	7	6
Hf	3.2	2.6	3.7	4.3	3.3	4.5	5.5	3.9	3.3	3.8	-
Pb	8.6	9.0	6.9	6.6	7.2	9.0	8.4	8.2	7.2	8.2	-
Th	1.9	1.5	1.5	1.7	1.7	1.8	2.2	1.5	2.1	2.4	-
U	0.7	0.6	0.6	0.8	0.7	0.5	0.6	0.9	0.5	0.7	-
La	9.57	9.60	11.8	13.7	13.1	14.1	14.0	11.9	12.0	14.7	-
Ce	22.2	21.8	28.8	31.2	29.7	32.1	33.4	29.4	28.1	34.1	-
Pr	2.98	3.06	3.90	4.23	4.04	4.53	4.52	3.95	3.60	4.53	-
Nd	13.0	13.1	17.8	17.8	20.1	19.7	18.8	17.7	17.6	19.7	-
Sm	2.99	3.00	4.13	4.28	4.02	4.61	4.67	4.14	4.08	4.78	-
Eu	1.55	1.2	1.40	1.21	1.35	1.40	1.26	1.26	1.30	1.58	-
Gd	3.47	2.70	4.68	4.54	4.61	5.45	5.35	4.55	4.93	5.82	-
Tb	0.44	0.50	0.57	0.65	0.61	0.75	0.77	0.61	0.46	0.77	-
Dy	3.04	2.70	3.76	3.82	4.13	4.18	4.09	3.73	3.79	4.53	-
Ho	0.59	0.60	0.74	0.77	0.98	0.93	0.85	0.73	0.65	0.95	-
Er	1.89	1.70	2.50	2.60	2.32	2.70	2.67	2.39	2.23	2.89	-
Tm	0.26	0.27	0.29	0.41	0.26	0.40	0.38	0.34	0.22	0.41	-
Yb	2.05	1.90	2.26	2.59	2.45	2.78	2.93	2.45	2.01	2.35	-
Lu	0.24	0.29	0.32	0.42	0.36	0.43	0.43	0.40	0.23	0.39	-

occasional olivine, and clear glass characterized by round, not stretched, vesicles (Fig. 6B). Bulk tephra major element oxide analysis (Table 4) indicates an andesitic composition (SiO_2 of 61 wt%), with lower TiO_2 (0.9 wt%), Na_2O (4.5 wt%), and K_2O (0.6 wt%) than Hudson tephra, while the tephra glass is rhyolitic (Fig. 7). This tephra has much lower concentrations (Table 6; Fig. 8) of Ti (2,594-4,156 ppm), Rb (17-24 ppm), Zr (122-160 ppm), Ba (233-295 ppm), La (9.6-14.0 ppm) and Yb (1.9-2.9 ppm).

TABLE 7. TRACE-ELEMENT COMPOSITIONS OF H2 AND H3 TEPHRA NEAR COCHRANE.

	H2				H3 (P2 1991 AS)	
	Cochrane		Elsewhere		Cochrane	Elsewhere
	Core	Core	Core	Core	Core	Outcrop
Lake	Edita	Maldonado	Mellizas	Espejo	Anómina	Aisen
core	0902A T4	0904B	1106B T2	1003A T3	0607A T1	
sample#	96-97 cm		56-64 cm	0-30 cm	5-6 cm	Phase 2
Lab #	CS-3003	CS1338	CS2401	CS1317/18	CS-3057	N&S 1998
Ti	6,859	6,893	7,030	6,712	8,057	7,553
Mn	1,084	972	1,026	996	1,290	1,316
Rb	58	64	56	62	56	48
Sr	326	307	341	347	406	377
Y	40	44	38	41	43	40
Zr	354	318	314	400	336	414
Nb	17	15	16	18	16	17
Cs	2.0	2.1	1.9	1.6	1.2	1.5
Ba	623	652	699	733	628	778
Hf	8.7	8.3	7.8	9.0	7.5	10.4
Pb	11.5	12.6	10.4	12.4	7.1	-
Th	7.7	7.5	5.8	6.9	5.2	6.8
U	1.7	1.9	1.3	1.5	1.4	-
La	43.4	39.8	40.0	41.3	38.0	41.8
Ce	88.3	85.4	85.3	91.2	86.3	85.6
Pr	11.5	10.4	10.7	10.8	10.7	-
Nd	45.2	41.6	43.5	43.2	43.7	43.2
Sm	9.52	8.85	9.09	8.90	9.40	8.78
Eu	2.76	2.78	3.24	2.63	2.79	2.36
Gd	11.3	9.65	11.4	9.66	9.86	-
Tb	1.37	1.19	1.42	1.28	1.36	1.25
Dy	7.47	6.94	7.12	7.54	7.84	-
Ho	1.49	1.35	1.45	1.46	1.50	-
Er	4.39	4.13	4.44	4.51	4.74	-
Tm	0.63	0.56	0.58	0.61	0.65	-
Yb	4.18	3.97	4.06	4.22	4.43	4.42
Lu	0.63	0.57	0.59	0.64	0.63	0.65

Their age, thickness and all these petrochemical characteristics indicate that they are the same MEN1 tephra identified by Naranjo and Stern (2004) further to the north along both the Simpson and Mañiguales Rivers northwest of Coyhaique (Aisén sample T-36, Table 6), by Weller *et al*. (2015) in cores near Coyhaique (Mellizos, Table 6), and by Stern *et al*. (2015) in cores from the upper Río Cisnes valley (Embudo, Table 6).

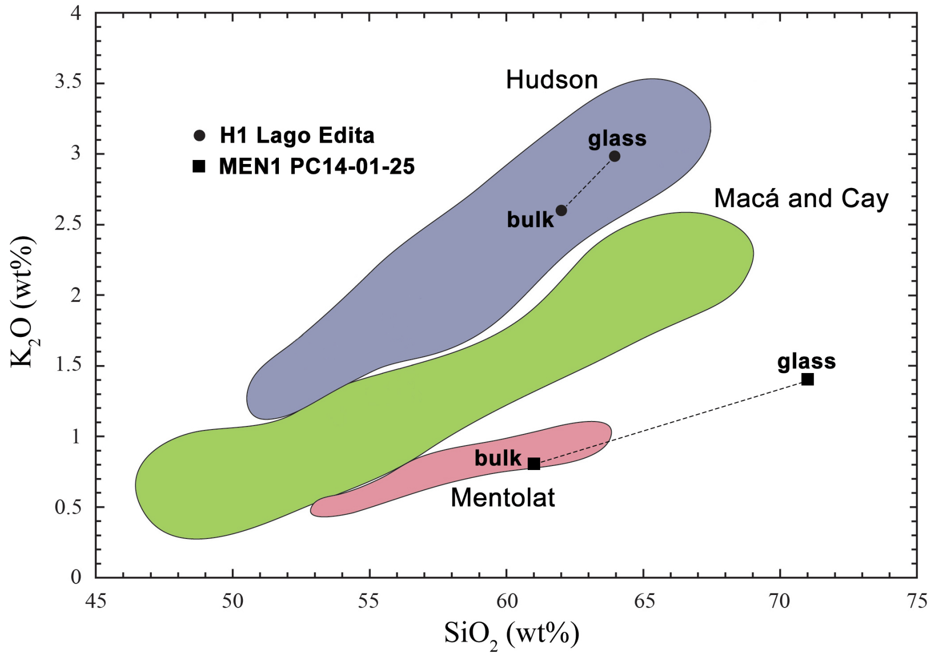

FIG. 7. SiO_2 *versus* K_2O for bulk tephra and tephra glass (Table 4) compared to fields for active volcanoes in the southern SVZ from previously published data (Futa and Stern, 1988; López-Escobar *et al*., 1993; Naranjo and Stern, 1998, 2004; D'Orazio *et al*., 2003; Gutiérrez *et al*., 2005; Kratzmann *et al*., 2009, 2010; Weller *et al*., 2014; Stern *et al*., 2015).

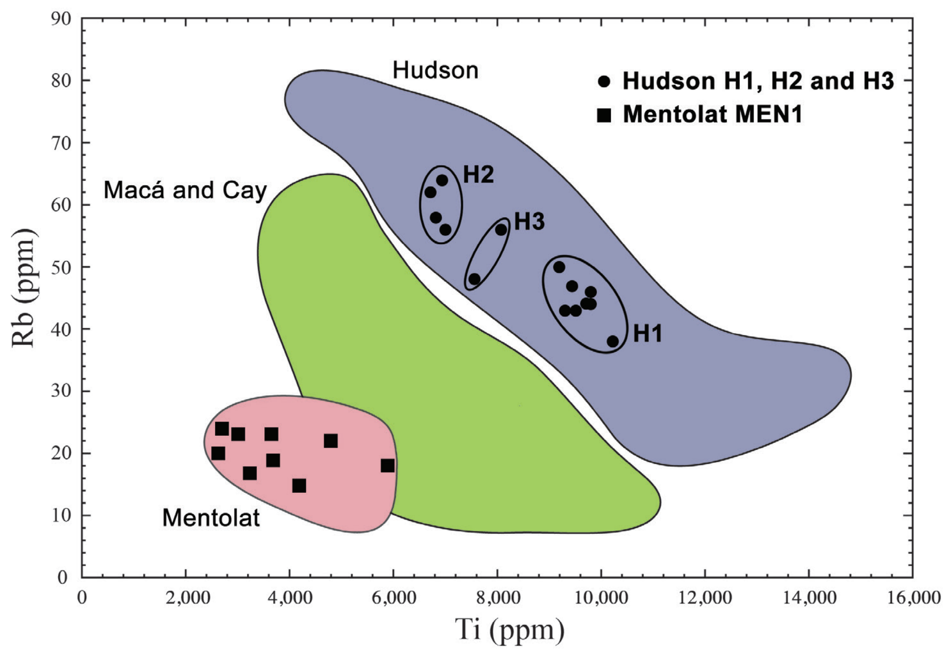

FIG. 8. Ti *versus* Rb for samples of tephra samples from near Cochrane derived from the Hudson (circles) and Mentolat (squares) volcanoes, compared to previously analyzed samples of lavas and tephra from Hudson, Macá, Cay and Mentolat (Futa and Stern, 1988; López-Escobar *et al*., 1993; Naranjo and Stern, 1998, 2004; D'Orazio *et al*., 2003; Gutiérrez *et al*., 2005; Kratzmann *et al*., 2009, 2010; Weller *et al*., 2014; Stern *et al*., 2015).

3.3. H2 and H3 tephra

Thin (<2 cm) Late Holocene tephra layers occur in some of the cores, but not in any of the trenches or outcrops. These are petrologically somewhat similar to H1 tephra, with plagioclase and pyroxene phenocrysts and brown glass with stretched vesicles, although the glass has a lighter color than H1 tephra glass. Bulk tephra also has higher Rb, Ba, Zr, La and Yb, but lower Ti contents than H1 tephra (Table 7; Fig. 8). Their late Holocene age, as indicated by their location relative to H1 tephra in the cores, and their chemistry and thickness is consistent with this tephra being a distal layer of the Hudson H2 eruption at approximately 4000 cal yrs BP (Naranjo and Stern, 1998).

Two separate cores (PC0607A and PC0607B) from Anónima bog contain a thin (1 cm) tephra layer near the very top of the cores, in sections T1 at 5-6 and 7-8 cm, respectively. The bulk tephra trace-element composition of this layer (Table 7; Fig. 8) is similar to other Hudson tephra, and this tephra is interpreted to be derived from the Hudson H3 eruption which occurred in 1991 AD (Scasso *et al*., 1994).

4. Discussion and Conclusions

4.1. H1 tephra distribution

H1 tephra layers range from 8 to 18 cm in thickness in the outcrop, trenches and cores we studied (Table 1). Gardeweg and Sellés (2013) also described two sections in outcrops from this general area (Fig. 2), one along the Tranquilo River (TCHA-10) and one near the Chacabuco bridge (TCHA-47), that based on their age determinations (Table 2) contain H1 tephra that ranges from 15 to 30 cm in thickness. The overall variability in thickness of all these multiple H1 tephra layers from the spatially closely associated sites near Cochrane suggest some significant degree of redistribution and/or thickening occurred during their deposition. Nevertheless, their widespread presence in this region as >8 cm layers is consistent with the suggestion of Gardeweg and Sellés (2013) that the 10 cm isopach for this eruption is probably larger and more extended in a southern direction than that drawn by Naranjo and Stern (1998). Figure 9 presents a new 10 cm isopachs for the H1 eruption based on these observations.

4.2. H1 eruption age

The seven bulk sediment AMS ages for H1 obtained from lake cores average 7,683±33 ^{14}C yrs BP (median probability age 8,440 cal yrs BP), and are somewhat older than the 14 AMS ages from surface (bog) deposits, which average 7,084±23 ^{14}C yrs BP (median probability age 7,891 cal yrs BP; Table 2). This systematic difference between ages of tephra determined from lake compared to bog deposits is statistically significant. Bertrand *et al*. (2012) demonstrated that bulk radiocarbon AMS age dates from lake sediments were 300 to 1,100 years older than true ages in some northern Patagonian lakes due to variable inputs of terrestrial organic carbon from the Holocene soils that cover the lake watersheds. However, our finding of nearly identical radiocarbon ages for H1 from multiple small, closed-basin lakes located at different elevations, in watersheds having contrasting slopes and degrees of soil development, however, argues against site-specific processes of soil erosion and redeposition for the striking radiocarbon synchrony among lakes.

Alternatively, dates from lacustrine environments may also be too old because of penetration of dense tephra into the water-saturated nepheloid layer and sediment-water interface in the bottom of lakes (Moreno *et al*., 2015). On the other hand, surface deposits are may be younger than true ages because humic acids percolate and contaminate these deposits. Finally ^{14}C ages may potentially be affected by ^{14}C reservoir effects. Ingram and Southon (1996), Taylor and Berger (1967), and more recently Carel *et al*. (2011) and Siani *et al*. (2010, 2013), determined ^{14}C reservoir effects of 200 to 600 years in the southeast Pacific ocean, but these reflect deep ocean circulation and are not directly applicable to the small, shallow, fresh-water, rain-fed lakes from which the tephra in this study were collected. Elbert *et al*. (2013) evaluated ^{14}C reservoir effects in two similar small lakes, Castor and Escondida, near Coyahique and found none. For Castor lake, ^{14}C reservoir effects were assessed using a paired measurement on bulk organic fraction and on a syndepositional terrestrial leaf macrofossil, which yielded identical ages. For Escondida lake potential reservoir effects were evaluated and discarded by parallel ^{14}C measurements of syndepositional diagnostic tephra layers which yielded similar ages in both lakes.

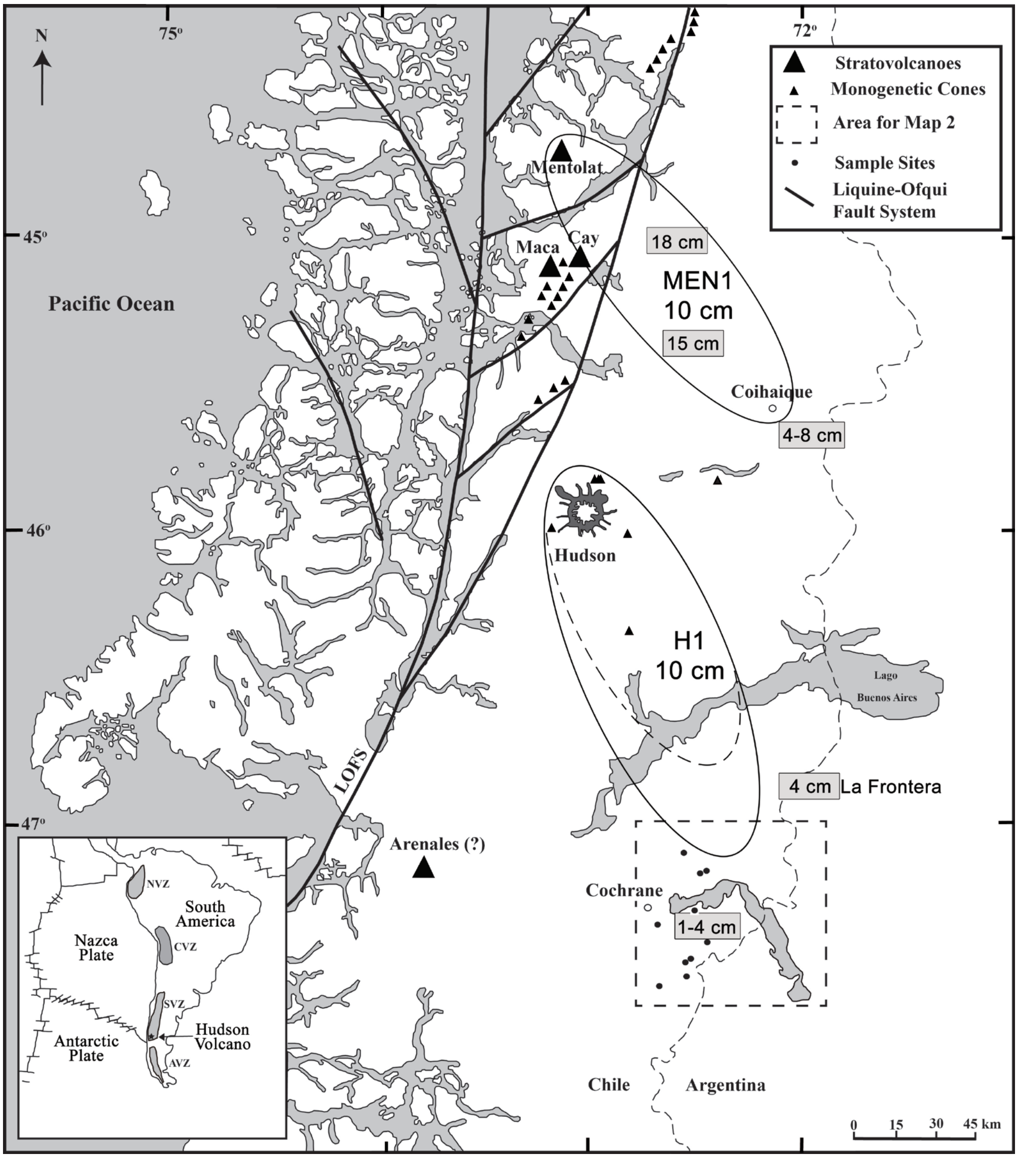

FIG. 9. A revised 10 cm isopach (solid lines) for the Hudson H1 eruption compared to that originally drawn (dashed line) by Naranjo and Stern (1998). The new isopach is based on the thickness of tephra in sections near Cochrane (Table 1), including those described by Gardeweg and Sellés (2013). Also shown is a tentative 10 cm isopach for MEN1 based on the distribution of MEN1 tephra (thickness given in small grey boxes) from cores and trenches near Cochrane (Table 1) and elsewhere, including from outcrops northwest of Coyhaique (Naranjo and Stern, 2004), eight lake cores near Coyhaique (Stern *et al*., 2013; Weller *et al*., 2014, 2015), and in a core at La Frontera, Argentina (McCulloch *et al*., 2014). MEN1 also occurs as diffuse 5 cm layers in cores from the upper Río Cisnes valley east of the volcano (Stern *et al*., 2015).

The new averages for AMS ages only from lake and surface deposits are both somewhat older than the most recent previously published age estimate for the H1 eruption of 6,890±100 ^{14}C yrs BP (median probability age 7,698 cal yrs BP; Stern, 2008; Prieto *et al*., 2013), which was based dominantly on conventional radiocarbon ages for samples from bog deposits. Although the total range of the different AMS ages from lakes and bogs compared to the conventional ages from bogs are overall relatively small (<700 years or <10% of the approximate >8,000 cal year BP age for H1), further refinements of the age of the H1 eruption is of interest, since this was the largest Holocene eruption in the southern Andes during the Holocene (Stern, 1991, 2004, 2008; Naranjo and Stern, 1998), and it produced a widely distributed tephra layer that has been used as a chronologic marker for numerous paleoclimate (Waldmann *et al*., 2009; Unkel *et al*., 2010; Borromei *et al*., 2010; Bjork *et al*., 2012; Villa-Martínez *et al*., 2012; Menounos *et al*., 2013) and archaeological studies (Prieto *et al*., 2013) in southern Patagonia.

4.3. MEN1 tephra age

The eight new ages for MEN1 from lake cores average 6,872±23 ^{14}C yrs BP (median probability age 7,689 cal yrs BP; Table 3), and are also, as for H1, somewhat older than the average for surface samples (median probability age 7,471 cal yrs BP), which includes one conventional radiocarbon age determined by Naranjo and Stern (2004). These ages are consistent with the occurrence of MEN1 only a few tens of centimeters above the older Hudson H1 tephra in the cores and trenches (Figs. 4 and 5).

4.4. MEN1 tephra source

Naranjo and Stern (2004) attributed the MEN1 tephra to an eruption of Mentolat based on a poorly constrained 10 cm isopach and geochemical data for one sample of this tephra which had low K_2O content relative to the products with similar SiO_2 erupted from other southernmost SVZ volcanoes (Maca, Cay and Hudson). The new major and trace-element geochemical data for this tephra are consistent with the conclusion that the source of this tephra is the Mentolat volcano. Basically, the few samples of lavas analyzed from Mentolat (López-Escobar *et al*., 1993), and all the MEN1 tephra samples (Table 6), have relatively low K_2O, Ti, Rb and Sr for samples with similar silica content erupted from other volcanoes in the southernmost SVZ (Figs. 7 and 8; Stern *et al*., 2015). Figure 9 summarizes the regional distribution in cm thickness of MEN1 tephra and presents a new, but still tentative, 10 cm isopach for this eruption. The area of this isopach is only a bit smaller than that within the 10 cm isopach of the 1932 AD eruption of Quizapu, which erupted 9.5 km^3 of pyroclastic material (Hildreth and Drake, 1992), but large enough to suggest an eruptive volume of at least 5 km^3 or greater. Although not as large as H1, MEN1 was still a reasonably large eruption, which if it were to happen again today could have a significant impact for local population centers such as Puerto Cisnes, Coyhaique and Cochrane.

4.5. H2 distribution

Gardeweg and Sellés (2013) describe a 45 cm thick orange tephra layer (TCHA-5B) along the south shore of Lago Cochrane, which they attribute to Hudson based on chemical data, and which they date as between 3,620±40 and 4,180±40 ^{14}C yrs BP. These ages are consistent with this being the late Holocene Hudson H2 tephra, but the thickness far exceeds the thickness of H2 tephra found in the lake cores in this region (~2 cm; Fig. 5), as well as the numerous outcrops previously used to determine isopachs for this eruption (Naranjo and Stern, 1998). We suggest instead that, based on its color and its thickness, this is not H2 tephra, but rather that the ages are incorrect, and that this is H1 tephra greatly thickened as a result of southward directed winds blowing tephra across the surface of Lago Cochrane during and after the H1 eruption.

4.6. H3 1991 AD tephra distribution

The presence of a 1-2 cm thick layer of H3 tephra at the top of the Anónima bog cores is consistent with the isopach distribution of H3 tephra as determined by Scasso *et al*. (1994).

4.7. Arenales volcano

No tephra evidence for the existence of the proposed Arenales volcano has been found in the sections studied, and we suggest that the Arenales volcano may not, in fact, exist, or alternatively that it has not had a moderate to large explosive eruption in the last 15,000 years.

Acknowledgements

We thank Á Amigo for many constructive comments that helped improve the final manuscript. This research was funded by Fondecyt grants #1080485, #1121141 and FONDAP 15110009, Fundación Fondecyt de Iniciación grant #11121280, CEQUA, and ICM grants P05-002 and NC120066.

References

Bertrand, S.; Araneda, A.; Vargas, P.; Jana, P.; Fagel, N.; Urrutia, R. 2012. Using the N/C ratio to correct bulk radiocarbon ages from lake sediments: Insights from Chilean Patagonia. Quaternary Geochronology 12: 23-29.

Björck, S.; Rundgren, M.; Ljung, K.; Unkel, I.; Wallin, A. 2012. Multi-proxy analyses of a peat bog on Isla de los Estados, easternmost Tierra del Fuego: a unique record of the variable Southern Hemisphere Westerlies since the last deglaciation. Quaternary Science Reviews 42: 1-14.

Borromei, A.M.; Coronato, A.; Franzén, L.G.; Ponce, J.F.; López-Sáez, J.A.; Maidana, N.; Rabassa, J.; Candel, M.S. 2010. Multiproxy record of Holocene paleoenvironmental change, Tierra del Fuego, Argentina. Palaeogeography, Palaeoclimatology, Palaeoecology 286: 1-16.

Carel, M.; Siani, G.; Delpech, G. 2011. Tephrostratigrapy of a deep-sea sediment sequence off the south Chilean margin: New insight into the Hudson volcanic activity since the last glacial period. Journal of Volcanology and Geothermal Research 208: 99-111.

D'Orazio, M.; Innocenti, F.; Manetti, P.; Tamponi, M.; Tonarini, S.; González-Ferrán, O.; Lahsen, A. 2003. The Quaternary calc-alkaline volcanism of the Patagonian Andes close to the Chile triple junction: geochemistry and petrogenesis of volcanic rocks from the Cay and Maca volcanoes (~45°S, Chile). Journal of South American Earth Sciences 16 (4): 219-242.

Elbert, J.; Wartenburg, R.; von Gunten, L.; Urrutia, R.; Fisher, D.; Fujak, M.; Hamann, Y.; Greber, N.D.; Grosjean, M. 2013. Late Holocene air temperature variability reconstructed from the sediments of Laguna Escondida, Patagonia Chile. Palaeogeography, Palaeoclimatology and Palaeoecology 396: 482-492.

Futa, K.; Stern, C.R. l988. Sr and Nd isotopic and trace element compositions of Quaternary volcanic centers of the southern Andes. Earth and Planetary Science Letters 88: 253-262.

Gardeweg, M.; Sellés, D. 2013. Tephrochronology from Villa Castillo to Lago O'Higgens, Aysenm Chile: New insights on the 6,700 and 3,600 years BP eruptions of Hudson Volvano. Bollettino di Geofisica Teorica ed Applicata 54 (Supplement 2): 155-157.

Gutiérrez, F.; Gioncada, A.; González-Ferrán, O.; Lahsen, A.; Mazzuoli, R. 2005. The Hudson volcano and surrounding monogenetic centres (Chilean Patagonia): an example of volcanism associated with ridge-trench collision environment. Journal of Volcanology and Geothermal Research 145: 207-233.

Hermanns, Y.M.; Biester, H. 2011. A Holocene record of mercury accumulation in a pristine lake in Southernmost South America (53°S): climatic and environmental drivers. Biosciences Discussion 8: 6555-6588.

Hildreth, W.; Drake, R.E. 1992. Volcán Quizapu, Chilean Andes. Bulletin of Volcanology 54: 93-125.

Hogg, A.G.; Hua, Q.; Blackwell, P.G.; Niu, M.; Buck, C.E.; Guilderson, T.P.; Heaton, T.J.; Palmer, J.G.; Reimer, P.J. 2013. SHCAL13 Southern Hemisphere Calibration, 0-50,000 years cal BP. Radiocarbon 55 (4): 1889-1903.

Ingram, B.L.; Southon, J.R. 1996. Reservoir ages in eastern pacific coastal and estuarine waters. Radiocarbon 38 (3): 573-582.

Kratzmann, D.J.; Carey, S.; Scasso, R.A.; Naranjo, J.A. 2009. Compositional variations and magma mixing in the 1991 eruptions of Hudson volcano, Chile. Bulletin of Volcanology 71 (4): 419-439.

Kratzmann, D.J.; Carey, S.; Scasso, R.A.; Naranjo, J.A. 2010. Role of cryptic amphibole crystallization in magma differentiation at Hudson volcano, Southern Volcanic Zone, Chile. Contributions to Mineralogy and Petrology 159: 237-264.

Lliboutry, L. 1999. Glaciers of the Wet Andes. *In* Satellite Image Atlas of Glaciers of the World, South America. (Williams, R.J.Jr.; Ferringo, J.G.; editors). United States Geological Survey, Professional Papers 1386-I; http://pubs.usgs.gov/prof/p1386i/index.html (last visit 05-01-2016).

López-Escobar, L.; Kilian, R.; Kempton, P.; Tagiri, M. l993. Petrology and geochemistry of Quaternary rocks from the southern volcanic zone of the Andes between 41°30' and 46°00'S, Chile. Revista Geológica de Chile 20 (1): 33-55. doi: 10.5027/andgeoV20n1-a04.

Menounos, B.; Clague, J.J.; Osborn, G.; Davis, P.T.; Ponce, F.; Goehring, B.; Maurer, M.; Rabassa, J.; Coronato, A.; Marr, R. 2013. Latest Pleistocene and Holocene glacier fluctuations in southernmost Tierra del Fuego, Argentina. Quaternary Science Reviews 77: 70-79.

McCulloch, R.; Figuerero-Torres, M.J.; Mengoni-Goñalons, G.L.; Barclay, R. 2014. Un registro Holocénico de cambios ambientales dinámicos y cronología cultural de Monte Zeballos-Paso Roballos, Santa Cruz, Patagonia central. *In* Jornadas de Arqueología de la Patagonia, No. 9, Libro de Resumenes: p. 4. Coyhaique.

Moreno, P.I.; Alloway, B.V.; Villarosa, G.; Outes, V.; Henríquez, W.I.; De Pol-Holz, R.; Pearce, N.J.G. 2015. A past-millennium maximum in postglacial activity from Volcán Chaitén, southern Chile. Geology 43: 47-50.

Naranjo, J.A.; Stern, C.R. 1998. Holocene explosive activity of Hudson Volcano, southern Andes. Bulletin of Volcanology 59 (4): 291-306.

Naranjo, J.A.; Stern, C.R. 2004. Holocene tephrochronology of the southernmost part (42°30'-45°S) of the Andean Southern Volcanic Zone. Revista Geológica de Chile 31 (2): 225-240. doi: 10.5027/andgeov31n2-a03

Prieto, A.; Stern, C.R.; Estévez, J.E. 2013. The peopling of the Fuego-Patagonian fjords by littoral hunter-gatherers after the mid-Holocene H1 eruption of the Hudson volcano. Quaternary International 317: 3-13.

Saadat, S.; Stern, C.R. 2011. Petrochemistry and genesis of olivine basalts from small monogenetic parasitic cones of Bazman stratovolcano, Makran arc, southeastern Iran. Lithos 125: 609-617.

Scasso, R.A.; Corbella, H.; Tiberi, P. l994. Sedimentological analysis of the tephra from the 12-15 August l991 eruption of Hudson volcano. Bulletin Volcanology 56: 121-132.

Siani, G.; Colin, C.; Mechel, E.; Carel, M.; Richter, T.; Kissel, C.; Dewilde, F. 2010. Late Glacial to Holocene terrigenous sediment record in the Northern Patagonian margin: paleoclimate implications. Palaeogeography, Palaeoclimatology, Palaeoecology 297: 26-36.

Siani, G.; Michel, E.; De Pol-Holz, R.; DeVries, T.; Lamy, F.; Carel, M.; Isguder, G.; Dewilde, F.; Lourantou, A. 2013. Carbon isotope records reveal precise timing of enhanced Southern Ocean upwelling during the last deglaciation. Nature Communications 4 (2758): 1-9. doi: 10.1038/ncomms3758.

Stern, C.R. 1991. A mid-Holocene tephra on Tierra del Fuego derived from the Hudson volcano (46ºS): Evidence for a large explosive eruption. Revista Geológica de Chile 18: 139-146. doi: 10.5027/andgeoV18n2-a04.

Stern, C.R. 2004. Active Andean volcanism: its geologic and tectonic setting. Revista Geológica de Chile 31 (2): 161-206. doi: 10.5027/andgeoV31n2-a01.

Stern, C.R. 2008. Holocene tephrochronology record of large explosive eruptions in the southernmost Patagonian Andes. Bulletin of Volcanology 70 (4): 435-454.

Stern, C.R.; López-Escobar, L.; Moreno, H.; Clavero, J.; Naranjo, J.A.; Parada, M.A.; Skewes, M.A. 2007. Chilean Volcanoes. *In* The Geology of Chile (Moreno, T.; Gibbons, W.; editors), Geologic Society of London, Chapter 5: 149-180.

Stern, C.R.; Moreno, P.I.; Henríque, W.I.; Villa-Martínez, R.P.; Sagredo, E.; Aravena, J.C. 2013. Tehrochronolgy in the area around Cochrane, southern Chile. Bollettino di Geofisica Teorica ed Applicata 54, Supplement 2: 199-202.

Stern, C.R.; de Porras, M.E.; Maldonado, A. 2015. Tephrochronology of the upper Río Cisnes valley (44°S), southern Chile. Andean Geology 42 (2): 173-189. doi: 10.5027/andgeoV42n2-a02.

Stuiver, M.; Reimer, P.J.; Braziunas, T.F. 1998. High-precision radiocarbon age calibration for terrestrial and marine samples. Radiocarbon 40 (3): 1127-1151.

Taylor, R.; Berger, R. 1967. Radiocarbon content of marine shells from the pacific coasts of Central and South America. Science 158: 1180-1182.

Unkel, I.; Fernández, M.; Björk, S.; Ljung, K.; Wohlfarth, B. 2010. Records of environmental changes during the Holocene from Isla de los Estados (54.4°S), southeastern Tierra del Fuego. Global and Planetary Change 74: 99-113.

Vargas, G.; Rebolledo, S.; Sepúlveda, S.A.; Lahsen, A.; Thiele, R.; Townley, B.; Padilla, C.; Rauld, R.; Herrera, M.J.; Lara, M. 2013. Submarine earthquake rupture, active faulting and volcanism along the major Liquiñe-Ofque Fault Zone and implications for seismic hazard assessment in the Patagonian Andes. Andean Geology 40 (1): 141-171. doi: 10.5027/andgeoV40n1-a07.

Villa-Matínez, R.; Moreno, P.I.; Valenzuela, M.A. 2012. Deglacial and postglacial changes on the eastern slopes of the central Patagonian Andes (47°S). Quaternary Science Reviews 32: 86-99.

Waldmann, N.; Ariztegui, D.; Anselmetti, F.S.; Austin Jr, J.A.; Stern, C.R.; Moy, C.M.; Recasens, C.; Dunbar, R. 2009. Southward migration and strengthening of the Southern Hemisphere Westerlies during the Mid-Holocene: evidence from Tierra del Fuego, Patagonia. Journal of Quaternary Sciences 24: 1-14.

Weller, D.; Miranda, C.G.; Moreno, P.I.; Villa-Martínez, R.; Stern, C.R. 2014. The large late-glacial Ho eruption of the Hudson volcano, southern Chile. Bulletin of Volcanology 76: 831-849.

Weller, D.; Miranda, C.; Moreno, P.I.; Villa-Martínez, R.; Stern, C.R. 2015. Tephrochronology of the southernmost Andean Southern Volcanic Zone, Chile. Bulletin of Volcanology 77: 107. doi: 10.1007/s00445-015-0991-2

Wright, H.E. Jr. 1967. A square-rod piston sampler for lake sediments. Journal of Sedimentary Petrology 37: 975-976.

Manuscript received: June 04, 2015; revised/accepted: September 25, 2015; available online: September 28, 2015.